



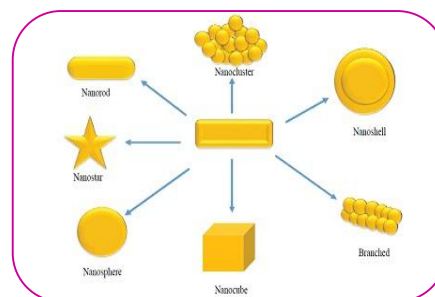
SPIN POLARIZATION OF GOLD NANOPARTICLES IN AC FIELDS

Arvindkumar Singh¹, Amitkumar² and Dr. Ak Singh³

¹Research scholar ,Dept. physics ,LNMU,Darbhanga.

²Research scholar ,Dept. physics ,LNMU,Darbhanga.

³Dept. physics, GD College ,Begusari.



ABSTRACT:

Optical and catalytic properties appear as the size of a bulk material is reduced to the nanometer scale when one encounters the so-called size effects. Upon reducing the size of a particle to a few hundred of nanometers, the first size effect encountered is the surface effect, where the ratio between the numbers of surface and core atoms is no longer ignorable, so that the surface properties are revealed together with the bulk behavior. Small size effect marks the effect of disruption of the lattice periodicity at the particle surface, where phonon softening and additional low-frequency phonon modes are commonly seen. These effects can be expected for particles of a few ten nanometers in diameter. Quantum confinement restricts the spatial motions of electrons and splits the electronic energy bands into discrete narrow sub-bands. It governs the electronic behavior of particles smaller than 10 nm in diameter.

KEYWORDS: Au nanoparticle; moment; field induced, nanometer, nano-sized ,particles, magnetization.

1.INTRODUCTION

Novel electronic, optical and catalytic properties appear as the size of a bulk material is reduced to the nanometer scale when one encounters the so-called size effects. There are three size effects that have been identified which can significantly alter the electron and lattice structures of a particle. Upon reducing the size of a particle to a few hundred of nanometers, the first size effect encountered is the surface effect, where the ratio between the numbers of surface and core atoms is no longer ignorable, so that the surface properties are revealed together with the bulk behavior. Small size effect marks the effect of disruption of the lattice periodicity at the particle surface, where phonon softening and additional low-frequency phonon modes are commonly seen [1,2]. Most of the studies made on the magnetic behavior of Au NPs were performed using polymer-capped particles, rarely with bare Au NPs. However, the physical behavior of capped NPs can be significantly altered by the interactions between the Au NPs and the capping agents. In the present article, we aim to discuss the magnetic properties of capping-free Au NPs, with emphasis on the property changes

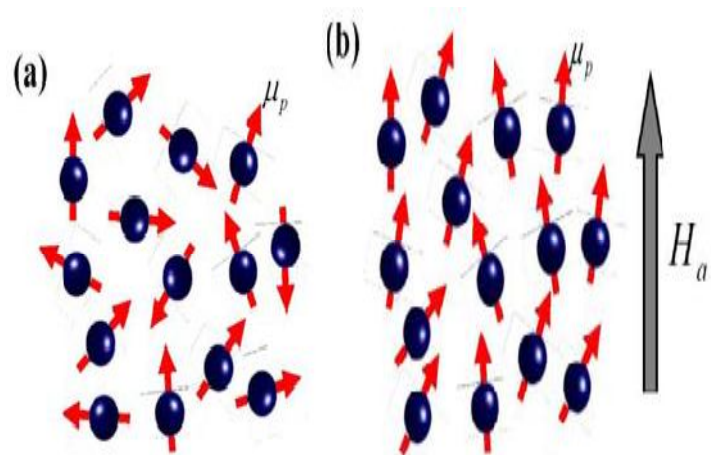
originating from size effects while avoiding the complications that may arise from the capping agents[3]. Our previous studies made on a 4 nm capping-free Au particle assembly reveal paramagnetic, rather than diamagnetic, responses to a driving ac magnetic field. The temperature profile of the average particle moment of a 3.5 nm capping-free Au powder assembly reveal a ferrimagnetic-like spin arrangement, where the moments of the inner and surface atoms point in opposite directions[4,5]. Magnetization and ac magnetic susceptibility are the physical parameters commonly used to reveal the macroscopic magnetic characteristics of magnetic systems. The former measures the amount of the magnetic moment in the system, whereas the latter picks up the magnetic response of the system to an driving ac magnetic field [6]. The magnetization M is measured by detecting the induced voltage in the detector coils as the sample moves through them. For ac magnetic susceptibility measurements, the sample is subjected to a weak driving ac magnetic field with the selected frequency and field strength. The responses of the system are detected using two identical sensing coils connected in opposition. Both the in-phase component χ' and the out-of-phase component χ'' can be measured simultaneously. We note that χ' measures the response of the system to the driving field, while χ'' reflects the losses of the driving field to the system. The NPs are very loosely packed for these measurements, so that they reveal mainly the magnetic responses from individual NPs without significant contributions from interparticle interactions. The packing fraction f , which marks the ratio between the mass densities of the NP assembly in the holder and that of bulk Au, is used to quantify the average interparticle separation that signals the significance of interparticle interactions in the nanoparticle assembly[7]. The packing fraction chosen for all NP powders used in the present studies is $\sim 6\%$, which corresponds to an average interparticle separation, from edge-to-edge, of 1.25 times the particle diameter. The holder produces a smooth temperature curve and a background signal that is $\sim 2\%$ of the signal from samples[8]. The net magnetization M at a finite temperature for a NP powder consisting of many individual well-separated (interaction-free) NPs, each carrying a net particle magnetic moment. The dimensionless permeability λ indicates the net effects from the magnetocrystalline anisotropy, molecular field, and applied magnetic field, such that λHa represents the magnetic field inside the NPs experienced by $\bar{\mu}_p$. This will be zero, when the NPs are naturally packed and the particle moments are randomly oriented, as illustrated in

Figure 1a. Under an applied magnetic field \bar{H}_a the tendency for the individual $\bar{\mu}_p$ to be aligned along the field direction increases [9]. The magnetic energy takes the form of $\mu p \lambda Ha$. The dimensionless permeability λ indicates the net effects from the magnetocrystalline anisotropy, molecular field, and applied magnetic field, such that λHa represents the magnetic field inside the NPs experienced by $\bar{\mu}_p$. This takes the form of $\lambda = 1 + (\mu_0 M_P^2 / 2K)$ for uniaxial spheres, where K is the energy density associated with magnetocrystalline anisotropy, μ_0 is the magnetic permeability of free space, and M_P is the spontaneous saturation magnetization[10,11]. According to the Boltzmann statistics, the competition between the magnetic

interaction energy $\mu_p \lambda H_a$ and the thermal agitation energy $k_B T$ gives rise to a Langevin profile for the dependency of M on H_a and $M_L(H_a, T) = M_P(T) L(x)$ where $M_P(T)$ indicates the saturation particle magnetization of the NP powder at a temperature T ,

$$L(x) \equiv \coth(x) - \frac{1}{x} \dots\dots\dots 1$$

is the Langevin function with $x \equiv \lambda \mu_p H_a / k_B T$, and k_B is the Boltzmann's constant. The Langevin $M_L(H_a, T)$ profile is understood to be a randomly oriented assembly of many interaction-free magnetic NPs with an average particle moment μ_p at a temperature T that are being aligned by the applied magnetic field, as illustrated in Figure 1b Schematic illustrations of the moment configuration of a nanoparticle assembly. Each carries a particle moment μ_p (a) without and (b) with the presence of an applied magnetic field H_a .



2. ZEEMANSPLIT MAGNETIZATION

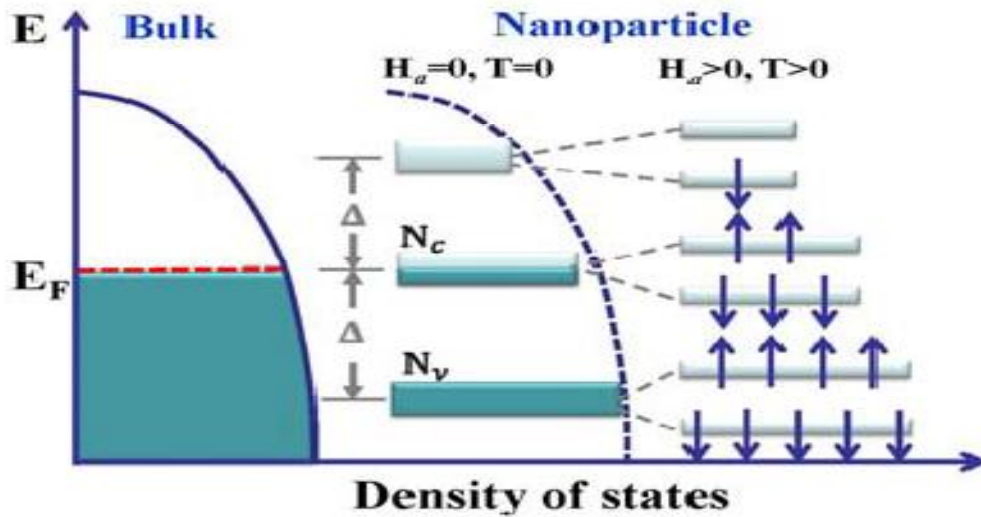
When the discrete nature of the electron level spacing becomes visible, magnetization contributed from the condensation of quantum-confined electrons into Zeeman split spin polarized states can also be induced by an applied magnetic field. This H_a -induced magnetization is mainly contributed from the conduction electrons. A schematic plot of the Zeeman split level spectrum near the Fermi level for quantum-confined electrons is shown in Figure 2, assuming that the level separations of the discrete spectrum take the same value of Δ . At a finite temperature, thermal excitations from conduction electrons into the first excited band and from the valence electrons into the conduction band are equally probable. It is then the available

density-of-states for excitations measure the contributions to the Zeeman magnetism. The induced magnetization of these quantum spins follows a Brillouin profile .where M_Z represents the induced saturation magnetization,

$$B_J(y) = \frac{2J+1}{2J} \operatorname{ctnh} \left[\frac{(2J+1)y}{2J} \right] - \frac{1}{2J} \operatorname{ctnh} \left(\frac{y}{2J} \right) \dots\dots\dots 2$$

The Brillouin function of order J , $y = g\mu_B\lambda Ha/kBT$, g is the Landeg-factor, and μ_B is the Bohr magneton. The Brillouin function reduces to a Langevin function when $J = \infty$ that is $B_\infty(y) = L(y)$, and it reduces to a hyperbolic tangent function when $J = 1/2$ that is $B_{1/2} = \tanh(y)$. Competition between thermal agitation and field alignment results in a Langevin type of magnetization curve $ML(Ha, T)$, whereas the thermal excitation of the valence and conduction electrons into Zeeman split spin polarized states gives rise to a Brillouin magnetization $MB(Ha, T)$. Although the thermal profile of the Brillouin function is different from that of the Langevin function, they look similar. Although the thermal profile of the Brillouin function is different from that of the Langevin function, they look similar.

Figure 2. Schematic illustrations of the density of states of bulk Au and the Zeeman split level spectrum near the Fermi level of quantum-confined electrons, assuming an even level separation Δ for the discrete spectrum.



3. SIZE DISPERSION DETECTION

Detecting the ultimate but extremely weak magnetic signals from a single NP is hardly achievable. The magnetic signals can be greatly enhanced by using a collection of NPs, but mono-dispersed powder is difficult to find. It has been shown that ignoring the influences from size dispersions of NP powders

can result in unphysical conclusions. In considering the magnetization from a NP powder, the contributions from particles of different sizes must be taken into account. The Langevin magnetization then takes the form of

$$M_L(H_a, T) = \sum_i n_i \mu_{pi} L\left(\frac{\mu_{pi} \lambda_i H_a}{k_B T}\right) = \sum_i n_i \mu_{pi} L\left(\frac{\mu_{pi} \lambda H_a}{k_B T}\right) \quad \dots\dots\dots 3$$

where n_i is the number of particles with a particle moment μ_{pi} , λ_i is the magnetic permeability of the corresponding particle that can be taken as a constant value λ for a narrow-dispersed powder. It is unphysical to extract all the parameters associated with the above expression from the observed $ML(H_a, T)$ unless the number of free parameters can be largely reduced. However, the stronger diamagnetic responses at lower temperatures are still evident, so that the net paramagnetic signals are smaller at lower temperatures. Curie-Weiss-like superparamagnetic responses are seen in the 3.5 nm Au-74 assembly. These χ' were collected without the presence of H_a , but reveal the responses of the particles to the driving magnetic field. One way to understand this behavior is that the Pauli paramagnetic responses are greatly enhanced in nano-sized particles, so that they overcome the weakened diamagnetic ones. It is known that the Pauli paramagnetic response is proportional to the density of states at the Fermi energy $g(\epsilon_F)$. The largely enhanced paramagnetic responses will require that $g(\epsilon_F)$ is also greatly increased, if there is no spontaneous magnetic component. Although $g(\epsilon_F)$ can be altered or even enhanced in nano-sized particles, it still hardly accounts for the three orders-of-magnitude enlargement in the Pauli paramagnetic responses. The existence of spontaneous magnetic moments in nano-sized Au particles is needed to understand the thermal characteristics of χ' . Magnetization is a physical quantity that measures the net magnetic moment of the system.

Magnetization measurement made on a multi-domain system is frequently performed with the presence of an H_a , which serves to align the magnetic moments of the domains along the field direction

4. CONCLUSIONS:

Many studies related to the magnetic properties of Au nanoparticles have been performed on polymer-capped Au nanoparticles. The present study, nevertheless, focuses on identifying the magnetic properties and the critical particle size for developing sizable spontaneous magnetic moments of bare Au nanoparticles. Seven sets of bare Au nanoparticle assemblies were fabricated employing the gas condensation method, which adopts a physical process involving the self-nucleation of atoms to form capping free Au nanoparticles. The resultant nanoparticles were no longer golden yellow but dark black, indicating that the absorption bands of the nanoparticles had blue shifted to the invisible region. The line profiles of X-ray diffraction peaks were used to determine the mean particle diameters and size distributions of the nanoparticle assemblies.

Although the moments developed in the Au nanoparticles are relatively weak, localized $5d$ holes do exist to reveal ferromagnetism. The paramagnetic behavior is associated with density of the $6s$ conduction electrons. The present observations involve both conduction $6s$ electrons and localized $5d$ holes.

REFERENCES

- [1]. Garitaonandia, J.S.; Insausti, M.; Goikolea, E.; Suzuki, M.; Cashion, J.D.; Kawamura, N.; Ohsawa, H.; de Muro, I.G.; Suzuki, K.; Plazaola, F.; *et al.* Chemically induced permanent magnetism in Au, Ag, and Cu nanoparticles: localization of the magnetism by element selective techniques. *Nano Lett.* **2008**, *8*, 661–667.
- [2]. Wu, C.-M.; Li, C.-Y.; Kuo, Y.-T.; Wang, C.-W.; Wu, S.-Y.; Li, W.-H. Quantum spins in icosahedral gold nanoparticles. *J. Nanopart. Res.* **2010**, *12*, 177–185
- [3]. Daniel, M.-C.; Astruc, D. Gold nanoparticles: Assembly, supramolecular chemistry, quantum-size-related properties, and applications toward biology, catalysis, and nanotechnology. *Chem. Rev.* **2004**, *104*, 293–346.
- [4]. Zhang, P.; Sham, T.K. Tuning the electronic behavior of Au nanoparticles with capping molecules. *App. Phys. Lett.* **2002**, *81*, 736–738.
- [5]. Zhang, P.; Sham, T.K. X-ray studies of the structure and electronic behavior of alkanethiolate-capped gold nanoparticles: The interplay of size and surface effects. *Phys. Rev. Lett.* **2003**, *90*, 245502.
- [6]. Jadzinsky, P.D.; Calero, G.; Ackerson, C.J.; Bushnell, D.A.; Kornberg, R.D. Structure of a thiolmonolayer-protected gold nanoparticles at 1.1 Å resolution. *Science* **2007**, *318*, 430–433.
- [7]. Carmeli, I.; Leitus, G.; Naaman, R.; Reich, S.; Vager, Z. Magnetism induced by the organization of self-assembled monolayers. *J. Chem. Phys.* **2003**, *118*, 10372–10375.
- [8]. Dutta, P.; Pal, S.; Seehra, M.S.; Anand, M.; Roberts, C.B. magnetism in dodecanethiol-capped gold nanoparticles: role of size and capping agent. *Appl. Phys. Lett.* **2007**, *90*, 213102.
- [9]. De la Venta, J.; Pucci, A.; FernándezPinel, E.; García, M.A.; de JuliánFernández, C.; Crespo, P.; Mazzoldi, P.; Ruggeri, G.; Hernando, A. Magnetism in polymers with embedded goldnanoparticles. *Adv. Mater.* **2007**, *19*, 875–877.
- [10]. López-Cartes, C.; Rojas, T.C.; Litrán, R.; Martínez-Martínez, D.; de la Fuente, J.M.; Penadés, S.; Fernández, A. Gold nanoparticles with different capping systems: An electronic and structuralXAS analysis. *J. Phys. Chem. B* **2005**, *109*, 8761–8766.
- [11]. Chi-Yen Li, Sunil K. Karna, Chin-Wei Wang and Wen-Hsien Li, Spin Polarization and Quantum Spins in Au Nanoparticles, *Int. J. Mol. Sci.* 2013, *14*, 17618-17642; doi:10.3390/ijms140917618